

Reynolds number effects on transition, turbulence intensity and axial-velocity decay rate of turbulent round jets

Ramanathan Varadharajan¹,

ABSTRACT

Numerical simulations of turbulent round jets, using explicit-filtered LES technique, are performed, for three different Reynolds numbers ($Re = 3600, 88000, 400000$), to understand the Reynolds number effect on subsonic jets with Mach number 0.9. Eighth-order compact schemes are used for spatial derivative estimation. Second order Runge-Kutta method is used for Time evolution of flow. One-parameter fourth-order compact filter is used for low-pass explicit filtering of transported variables. Decreased centreline axial velocity decay rate and reduced turbulence intensities are observed as jet Reynolds number increases. Jet spread-rate is observed to be independent of the Reynolds number. An early potential-core collapse and transition to turbulent regime is observed in jets with high Reynolds number, for same inflow turbulence seeding. Role of increased smaller length scales with increase in Reynolds number is analyzed. It is observed that behavior of turbulent round jets is similar to that of plane jets, irrespective of gain in dimensional freedom. Detailed discussions of the observations made from numerical experiments are presented.

Keywords: Round jet, Reynolds number effects, Subsonic flow, Large eddy simulation, Turbulence intensity, Transition .

INTRODUCTION

Turbulent round jets have been extensively studied, both experimentally and numerically, for their rich physics and applications. Applications include but not limited to, turbulent mixing for efficient combustion, industrial whistles, turbulent noise reduction in aircraft jets, etc., Thus the evolution of Mean flow and turbulence characteristics of a round jet are extensively researched and documented in literature. Notable works involve experiments performed by Panchapakesan, (Panchapakesan and Hussein et al, (Hussein et al. 1994) to understand mean-flow and turbulence in jets. Jonathan B. Freund, performed Direct numerical simulations of subsonic

¹Laboratory of Physical Chemistry & Soft Matter, Wageningen University & Soft Matter, 6708WE Wageningen, The Netherlands. E-mail: ramanathan.varadharajan@wur.nl

round jet at 0.9 Mach Number (Freund 2001) to determine the noise sources in a turbulent jet.

Fellouh *et al.* (Fellouah et al. 2009), proved the Reynolds dependence in mixing transition in near and intermediate-field regions of round jet using hot-wire measurements. Effect of Reynolds number and initial conditions on turbulent mixing was studied by Boersma (Boersma et al. 1998), Hussain (Hussain 1986), George (George 1989), Dimotakis (Dimotakis 2000), Xu *et al.* (Xu and Antonia 2002) and Uddin *et al.* (Uddin and Pollard 2002). A good review of works can be found in Ball *et al.* (Ball et al. 2012). Presence of Reynolds number effects on jet parameters for plane jets was initially reported by Xu *et al.* (Xu et al. 2013). Xu's experiments on plane jets shows decrease in centerline decay rates, spread rate with increase in Reynolds number till a critical point is achieved.

In this paper, an extension of the work for round jets is presented, as most of the reported studies on Reynolds number effects were performed on non-circular jets, because of their high mixing efficiency. It should be noted that the mixing efficiency of circular jets are not insignificant. It will be shown that for round jets, the dependence on Reynolds number is similar to that of plane jets. Article also documents the first attempt to study Reynolds number effects on turbulence using explicit-filtered LES technique. Numerical Methods are explained in Section: 2. An account on the jet inflow conditions used are provided in Section: 3. Computational domain used for various simulations are described in Section: 4. Section: 5 presents the results and discussions.

NUMERICAL METHOD

The flows considered is governed by the Navier-Stokes equations for compressible flow

$$\frac{\partial \rho}{\partial t} + \frac{\partial \rho u_i}{\partial x_i} = 0, \quad (1)$$

$$\frac{\partial \rho u_i}{\partial t} + \frac{\partial \rho u_i u_j}{\partial x_j} = -\frac{\partial p}{\partial x_i} + \frac{\partial \tau_{ij}}{\partial x_j}, \quad (2)$$

$$\frac{\partial \rho E}{\partial t} + \frac{\partial}{\partial x_j} [(\rho E + p)u_j] = \frac{\partial q_i}{\partial x_i} + \frac{\partial u_j \tau_{ij}}{\partial x_j}. \quad (3)$$

Here ρ is the density, u_i are Cartesian velocity components, p is pressure, E is the energy and $\rho E = (\rho u_k u_k)/2 + p/(\gamma - 1)$. q_i is the heat flux. The Prandtl Number was set to a constant value of 0.71. Shear stress

$$\tau_{ij} = \mu \left(\frac{\partial u_i}{\partial x_j} + \frac{\partial u_j}{\partial x_i} - \frac{2}{3} \left[\frac{\partial u_k}{\partial x_k} \right] \delta_{ij} \right), \quad (4)$$

where μ , the dynamic viscosity, was calculated from Sutherland's law

$$\mu = \frac{1.458 \times T^{1.5}}{(T + 110.0)}. \quad (5)$$

TABLE 1: Details of round jet simulations

Simulation	jet Details		Parameters	
	Reynolds Number	Grid (No.of.Div. in jet)	B_u	x_{jc}/r_0
J1G2a	3600	$386 \times 201 \times 201$ (10)	5.96	42.4
J2G1	88000	$226 \times 171 \times 171$ (08)	6.37	20.2
J2G2	88000	$386 \times 201 \times 201$ (10)	6.28	19.8
J3G1	400000	$226 \times 171 \times 171$ (08)	7.40	14.8
J3G2	400000	$386 \times 201 \times 201$ (10)	6.60	14.5
J3G3	400000	$291 \times 241 \times 241$ (12)	6.55	14.2
Lumley, 1993	11000	N.A.(Experiment)	6.06	—
Freund, 2001	3600	$640 \times 250 \times 160$ (55)	5.80	14.0

Since the flows considered are turbulent, the numerical solution was found as a large eddy simulation using the explicit filtering method. Detailed information of the numerical procedure are provided in R. Varadharajan(Varadharajan 2016) and S. Ganesh(Ganesh 2014). Essential requirements for this method are that a high resolution numerical method be used along with a high resolution low pass spatial filter applied to transported variables after every time step. This approach to LES has been used successfully, for several types of flows, by at least two other groups (Visbal and Rizzetta 2014) (Bogey and Bailly 2006). Here, a Cartesian grid was used with a 8th-order compact difference formula for spatial derivatives, split into a forward and a backward step extending the method of Hixon and Turkel(Hixon and Turkel 1998) (Hixon and Turkel 2000). Time-stepping was by a 2nd-order Runge-Kutta(RK2) scheme. A one-parameter fourth-order compact filter (Lele 1992) was applied with filter paramter $\alpha = 0.475$ in the stream-wise direction and 0.498 in the cross-stream directions.

Partially non-reflecting, characteristic boundary conditions developed by K. W. Thompson(Thompson 1987) (Thompson 1990) and adapted for compressible fluid flow, by S.K. Lele (Poinsot and Lele 1992), were specified at boundaries. A constant time-step estimated from a maximum CFL number of 0.075 was used.

The numerical method described above, including boundary treatments, combining non-reflecting conditions, stretched grid buffer zone, and anchoring inflow variables to target values was developed and tested for jet aeroacoustics studies, see S. Ganesh(Ganesh 2014). And later successfully tested to understand jet instability modes on Hartmann whistle, see R.Varadharajan *et al.*(Varadharajan et al. 2016)

JET INFLOW CONDITIONS

Round jet with thin shear layer is provided as inflow. Velocity profile of jet is defined by top-hat profile given below,

$$U = \frac{U_j}{2} + \frac{U_j}{2} \tanh\left(\frac{r_0 - r}{2\theta}\right) \quad (6)$$

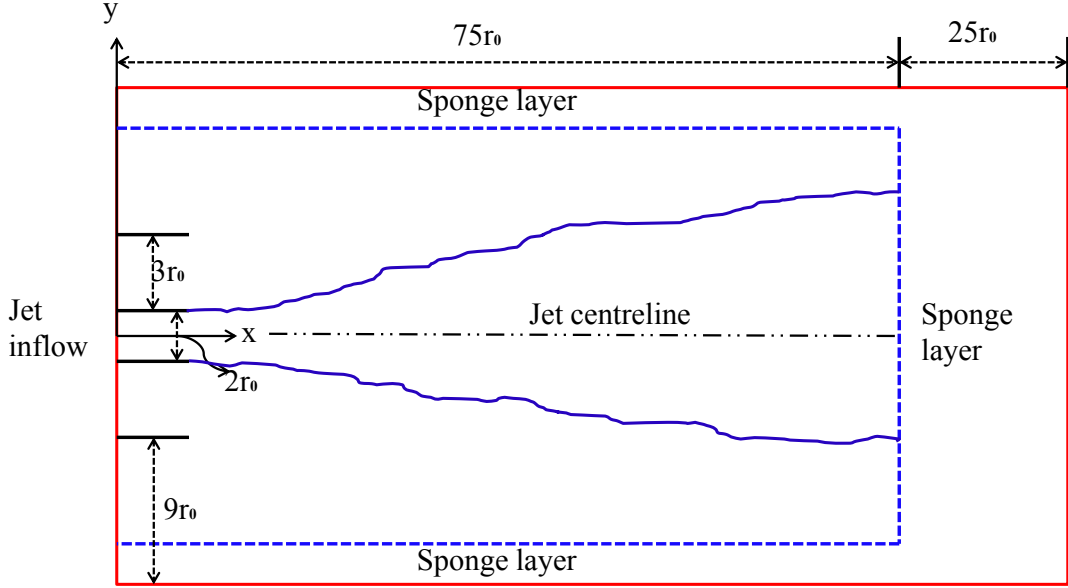


FIG. 1: Schematic of computational domain on the plane $z = 0$, in three-dimensional computational space. Sponge-layer is implemented to avoid spurious reflections from boundaries as shown in figure.

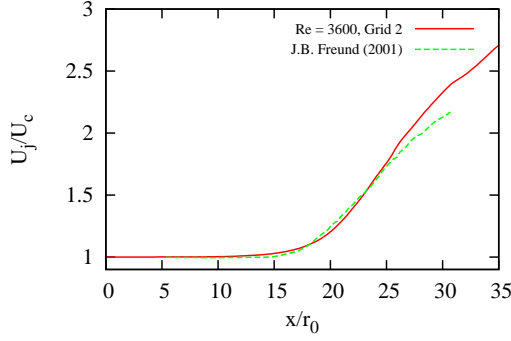
The above specified nozzle inflow condition represents jet with a thin laminar annular shear layer with radius r_0 and jet velocity U_j . Momentum thickness, $\theta = r_0/20$, is used for simulations. Mean inlet pressure is constant and maintained same as the ambient chamber pressure, $p_0 = 1823.85 \text{ Pa}$. Inlet density is determined using the Crocco-Busemann relationship. Ambient density, $\rho_0 = 0.022 \text{ kg/m}^3$ and inflow density, $\rho_{in} = 0.02564 \text{ kg/m}^3$ are used. Mach Number of simulated jets are set to constant value of 0.9. Random fluctuations are added to the stream-wise components at inflow to induce turbulence. The fluctuations are calculated as follows,

$$u'(\phi, t) = A \left[\sum_{i=1}^6 \sin(i\phi + \alpha_i + \psi_i t) + \sum_{i=7}^8 \sin(\psi_i t) \right]_{(x=0)} \quad (7)$$

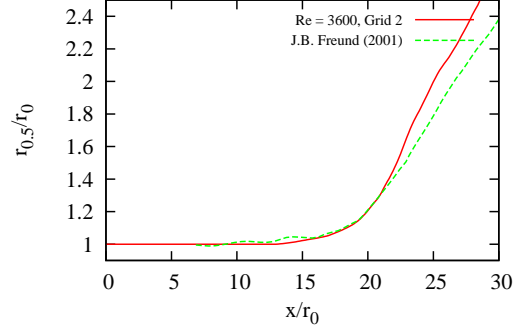
$$A = \frac{U_j}{1000} e^{(-128(\frac{r-R}{R})^2)} \quad (8)$$

where ϕ is the azimuthal angle. α_i and ψ_i are random numbers to generate random phase and frequencies. $R = 0.875r_0$ is used, providing with a gaussian function centered around R near nozzle lip. The perturbation u' is added at each step of RK2. The peak rms of the stream-wise velocity fluctuations are under 2% for all cases.

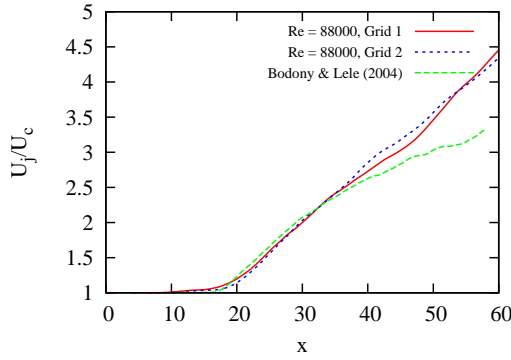
COMPUTATIONAL DOMAIN



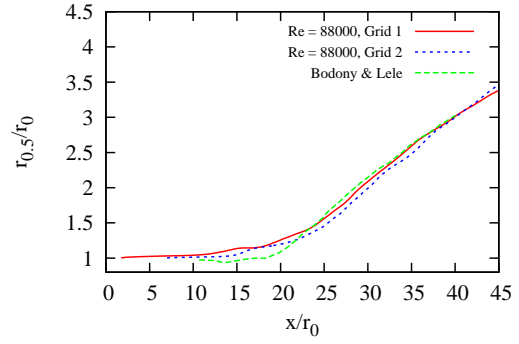
(a) $M=0.9$, $Re=3600$



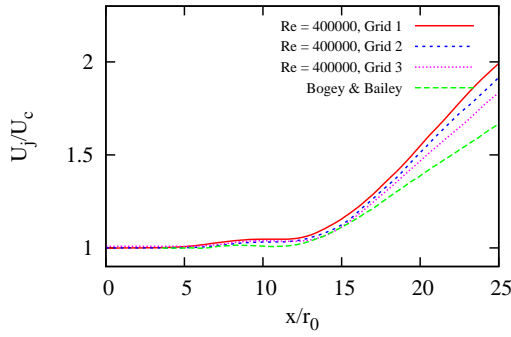
(b) $M=0.9$, $Re=3600$



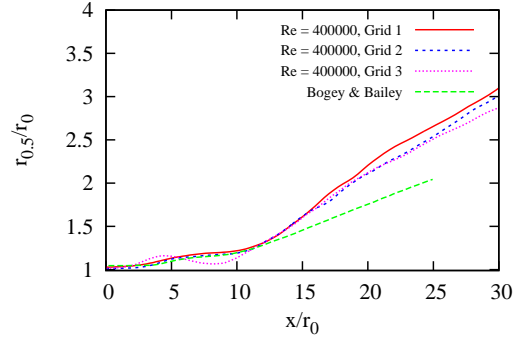
(c) $M=0.9$, $Re=88000$



(d) $M=0.9$, $Re=88000$



(e) $M=0.9$, $Re=400000$



(f) $M=0.9$, $Re=400000$

FIG. 2: Decay of centerline axial velocity & streamwise variation of jet half-width radius.

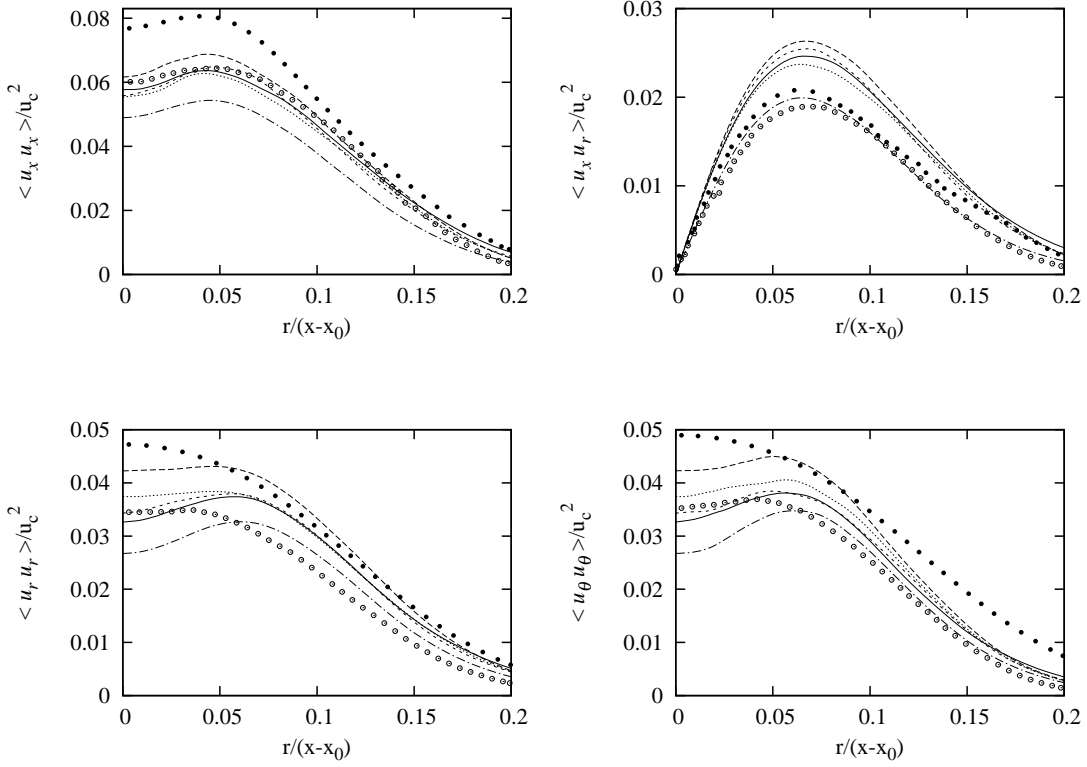


FIG. 3: Second moments of velocity: \bullet - Hussein *et al.* (1994); \circ - Panchapakesan & Lumley (1993); (----) - Re = 88000, Grid 1; (—) - Re = 88000, Grid 2; (- -) - Re = 400000, Grid 1; (····) - Re = 400000, Grid 2; (-·-·) - Re = 400000, Grid 3.

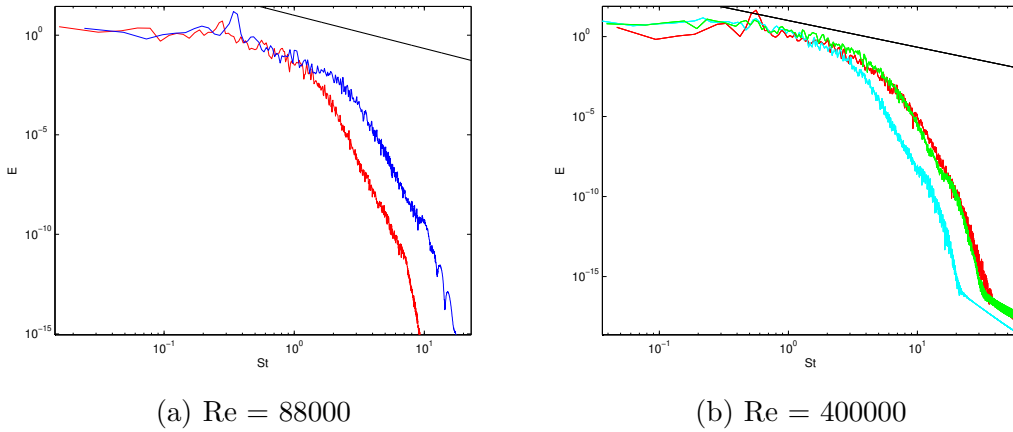


FIG. 4: Turbulent kinetic energy spectrum: Re = 88000: [(—) - Grid 1; (—) - Grid 2.] Re = 400000: [(—) - Grid 1; (—) - Grid 2; (—) - Grid 3.]; (—) - 5/3 slope line

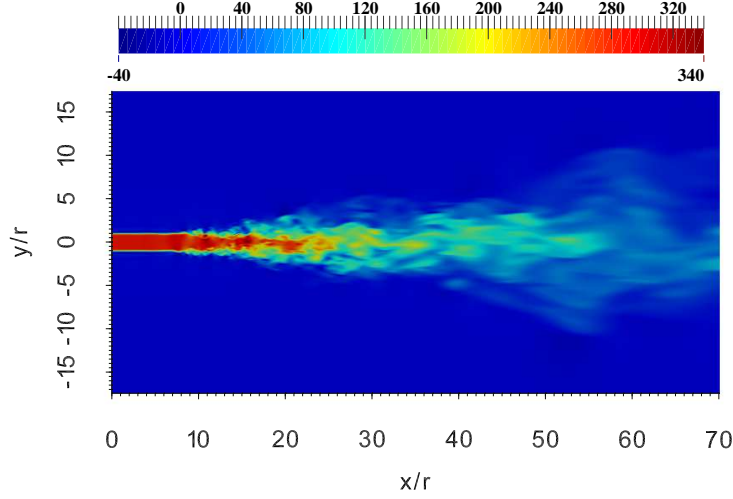


FIG. 5: Instantaneous contours of u -velocity at xy plane, $z = 0$. $Re = 4 \times 10^5$, showing potential-core collapse at $x = 14.5r_0$.

Computation domain used for simulations, are cartesian grids with x -axis along streamwise direction, y, z axis along cross-stream direction and origin located at jet centerline, is schematically represented in Figure 1. Three different grids with similar configuration are used as computational domain for all numerical simulations. 6 Simulations of Mach 0.9, $Re = 3600, 88000, 4 \times 10^5$ round jets, in three different grids, are performed to study the effect of Reynolds number.

Numerical grid with 16 uniform divisions in jet diameter, both in y and z direction, is called as Grid 1 (G1) throughout the article. Grid 1 is used to simulate two cases of jet with $Re = 88000, 4 \times 10^5$; From $y = \pm 4r_0$ and $z = \pm 4r_0$, 2% stretching in local Δy is used. Buffer region with 5 % stretching is used above $x = 75r_0$.

Numerical grid with 20 uniform divisions in jet diameter is called as Grid 2 (G2) throughout the article. Grid 2 is used to simulate three cases of jet with $Re = 3600$ (Grid 2a is used), $88000, 4 \times 10^5$; From $y = \pm 4r_0$ and $z = \pm 4r_0$, 2 % stretching in local Δy is used. Buffer region with 5 % stretching is used above $x = 75r_0$. Grid 2a is a variant of Grid 2, where the compression in the stream-wise direction is started at $x = 40r_0$ (which was the expected breakdown length for $Re = 3600$ case).

Numerical grid with 24 uniform divisions in jet diameter is called as Grid 3 (G3) throughout the article. Grid 3 is used to simulate single case of jet with $Re = 4 \times 10^5$; From $y = \pm 4r_0$ and $z = \pm 4r_0$, 2 % stretching in local Δy is used. Buffer region with 5 % stretching is used above $x = 75r_0$.

All three grids are compressed from $x = 6r_0$ and stretched after $x = 12r_0$ approximately. Grid is compressed to capture finer length scales in the near break down region. The region of compression is chosen based on expected break down point from previous numerical experiments. Compression and Stretching

parameters $r_c = 0.985$ and $r_s = 1.015$ represent the common ratio of compression and stretching respectively for all three grids. Grids described above are all developed as a function of jet radius r_0 .

SIMULATION RESULTS

Mean flow

In the numerical computations, there is an ambiguity in the definition of effective nozzle location as the computational domain doesn't include the nozzle. Therefore, virtual origin values of these simulations are matched to compare the simulation results with experimental and other computational works. Virtual origin values are obtained from the jet half-width radius. A linear fit for half-width radius is found in the self-similar region. This linear fit is extrapolated to find the virtual origin of the jets.

Self-Similarity (Pope 2001)(Benzi et al. 1993) states, downstream of jet breakdown and potential core collapse, the centerline velocity decays according to,

$$\frac{U_c}{U_j} = 2B_u \frac{r_0}{x - x_0} \quad (9)$$

where B_u is a measure of center-line axial-velocity decay rate. For the cases of simulations performed center-line axial velocity decay and Half-width radius are presented in Figure [2]. From Table 1, it can be observed that jets with higher Reynolds number has higher values of B_u . This shows that increase in Reynolds number causes decreased axial-velocity decay rate for turbulent round jets. It should also be noted that there isn't any significant variation of spread rate for different Reynolds numbers (Can be observed from jet halfwidth plots ($r_{0.5}/r_0$ vs. x/r_0) in Figure 2). In Figure 2(e,f) the slight deviation can be attributed to use of Cylindrical geometry by Bogey & Bailey (Bogey and Bailly 2006).

Turbulence

Downstream of the jet breakdown, jets become self similar. In the self similar region, the second moments of velocity are used to characterize the turbulence. Figure [3] shows that post-transition turbulence intensities decreases as Reynolds number increases. It can be observed that peak turbulence intensities are 33% lower for $Re = 400000$ when compared to $Re = 88000$ jets. This is similar to the observations of Xu *et al.* (Xu et al. 2013) for turbulent plane jets.

For all the simulations performed the Reynolds stress behavior is found to lie mostly within the profiles measured by Panchapakesan & Lumley (Panchapakesan and Lumley 1993) and Hussein *et al.* (Hussein et al. 1994). Slight deviation observed in near centerline region for some of the simulation is because the profiles were averaged in same range $x \geq 20r_0$, for all simulations, where some of the jets simulated are in transition or near-transition zone. Turbulence intensity profiles of J1G2a are not presented as the turbulence regime simulated for the case is small, and averaging in that span will not produce accurate results.

Energy spectra

Turbulent kinetic energy spectra, for simulations performed, are presented in Figure: [4]. Energy spectra is broad banded with the smallest scales having approximately 10^6 times less energy than greatest scale for all simulations. Turbulent kinetic energy of the simulated jets peaks around Strouhal Number, $St = 0.3 - 0.4$. Figure: [4a & 4b] shows that on grid refinement finer scales are captured accurately. Figure: [4] shows energy content of a fixed length-scale (Strouhal Number) increases with increase in Reynolds number. This is observed for smaller length-scales or higher strouhal numbers ($St \geq 0.5$), whereas the energy content in the highest length-scales or lower strouhal numbers remain independent of Reynolds number.

Flow organisation

Axial velocity contour of simulated jet is presented in Figure: [5]. Except for the differences in transition length, flow organisation remains the same for all simulations. Potential core collapse is observed at a range of $x = 14r_0 - 20r_0$ on an average for the simulations performed, with exception to $Re = 3600$ case. (where the potential core collapse is observed at $x = 39r_0$). It is observed that high Reynolds number jets have early transition (potential core collapse) for the same level of inflow turbulence.

SUMMARY

An early break-down to turbulence, decreased axial-velocity decay rates and decreased levels of turbulence intensities are observed with increase in Reynolds numbers for turbulent round jets. Eventhough more accurate numerical simulations for a range of Reynolds number are required to understand the effects, it could be observed that increased smaller length scales play a significant role in determining decay rates. Jet spread-rate though observed to remain almost independent of Reynolds number, it could be an artifact of cartesian grids inability to represent the physics. Simulations on a cylindrical grid, might reveal dependence of spread-rate on Reynolds number.

ACKNOWLEDGEMENTS

Author acknowledges the fruitful discussions with Dr. Joseph Mathew, Indian Institute of Science, Bangalore. Author is thankful to Dr. Subramanian Ganesh, General Electric, India for providing the basic computational algorithm. Computations were carried during author's stay at Indian Institute of Science, India, as a part of his graduate research on jet instability modes of Hartmann whistle. Analysis and findings published in this article were made after author moved to his new position at Wageningen University, The Netherlands.

REFERENCES

- Ball, C., Fellouah, H., and Pollard, A. (2012). “The flow field in turbulent round free jets.” *Progress in Aerospace Sciences*, 50, 1–26.
- Benzi, R., Ciliberto, S., Tripiccone, R., Baudet, C., Massaioli, F., and Succi, S. (1993). “Extended self-similarity in turbulent flows.” *Physical review E*, 48(1), R29.
- Boersma, B., Brethouwer, G., and Nieuwstadt, F. (1998). “A numerical investigation on the effect of the inflow conditions on the self-similar region of a round jet.” *Physics of Fluids (1994-present)*, 10(4), 899–909.
- Bogey, C. and Bailly, C. (2006). “Computation of a high Reynolds number jet and its radiated noise using large eddy simulation based on explicit filtering.” *Computers & Fluids*, 35(10), 1344 – 1358.
- Dimotakis, P. E. (2000). “The mixing transition in turbulent flows.” *Journal of Fluid Mechanics*, 409, 69–98.
- Fellouah, H., Ball, C., and Pollard, A. (2009). “Reynolds number effects within the development region of a turbulent round free jet.” *International Journal of Heat and Mass Transfer*, 52(17), 3943–3954.
- Freund, J. B. (2001). “Noise sources in a low-reynolds-number turbulent jet at mach 0.9.” *Journal of Fluid Mechanics*, 438, 277–305.
- Ganesh, S. (2014). “Large eddy simulation of free and impinging subsonic jets and their sound fields.” Ph.D. thesis, Indian Institute of Science, Department of Aerospace Engineering, Indian Institute of Science, Department of Aerospace Engineering.
- George, W. K. (1989). “The self-preservation of turbulent flows and its relation to initial conditions and coherent structures.” *Advances in turbulence*, 39–73.
- Hixon, R. and Turkel, E. (1998). *High-accuracy compact MacCormack-type schemes for computational aeroacoustics*. National Aeronautics and Space Administration, Lewis Research Center.
- Hixon, R. and Turkel, E. (2000). “Compact implicit maccormack-type schemes with high accuracy.” *Journal of Computational Physics*, 158(1), 51–70.
- Hussain, A. F. (1986). “Coherent structures and turbulence.” *Journal of Fluid Mechanics*, 173, 303–356.
- Hussein, H. J., Capp, S. P., and George, W. K. (1994). “Velocity measurements in a high-reynolds-number, momentum-conserving, axisymmetric, turbulent jet.” *Journal of Fluid Mechanics*, 258, 31–75.
- Lele, S. K. (1992). “Compact finite difference schemes with spectral-like resolution.” *Journal of computational physics*, 103(1), 16–42.
- Panchapakesan, N. and Lumley, J. (1993). “Turbulence measurements in axisymmetric jets of air and helium. part 1. air jet.” *Journal of Fluid Mechanics*, 246, 197–223.
- Poinsot, T. J. and Lele, S. (1992). “Boundary conditions for direct simulations of compressible viscous flows.” *Journal of computational physics*, 101(1), 104–129.
- Pope, S. B. (2001). “Turbulent flows.
- Thompson, K. W. (1987). “Time dependent boundary conditions for hyperbolic

- systems.” *Journal of computational physics*, 68(1), 1–24.
- Thompson, K. W. (1990). “Time-dependent boundary conditions for hyperbolic systems, ii.” *Journal of Computational Physics*, 89(2), 439–461.
- Uddin, M. and Pollard, A. (2007). “Self-similarity of coflowing jets: the virtual origin.” *Physics of Fluids (1994-present)*, 19(6), 068103.
- Varadharajan, R. (2016). “Les of free jets and jets impinging on cuboidal cavity.” M.S. thesis, Indian Institute of Science, Department of Aerospace Engineering, Indian Institute of Science, Department of Aerospace Engineering.
- Varadharajan, R., Kamin, M., Ganesh, S., and Mathew, J. (2016). “On the jet instability modes of hartmann whistle.” *Journal of Sound and Vibration*, (Submitted).
- Visbal, M. R. and Rizzetta, D. P. (2014). “Large-Eddy Simulation on Curvilinear Grids Using Compact Differencing and Filtering Schemes.” *ASME J. Fluids Engg.*, 124(December 2002).
- Xu, G. and Antonia, R. (2002). “Effect of different initial conditions on a turbulent round free jet.” *Experiments in Fluids*, 33(5), 677–683.
- Xu, M., Pollard, A., Mi, J., Secretain, F., and Sadeghi, H. (2013). “Effects of reynolds number on some properties of a turbulent jet from a long square pipe.” *Physics of Fluids (1994-present)*, 25(3), 035102.